Supporting Information

Genesis and effects of swapping bi-layers in hexagonal $GeSb_2Te_4$

Jiang-Jing Wang[1,‡], Jun Wang[1,‡], Hongchu Du[2], Lu Lu[3], Peter C. Schmitz[4], Johannes Reindl[5], Antonio M. Mio[5], Chun-Lin Jia[2,3], Evan Ma[1, 6], Riccardo Mazzarello[4], Matthias Wuttig[5,7], Wei Zhang*[,1]

[1] Center for Advancing Materials Performance from the Nanoscale, State Key Laboratory for Mechanical Behavior of Materials, Xi'an Jiaotong University, Xi'an 710049, China

[2] Peter Grünberg Institute and Ernst Ruska-Centre for Microscopy and Spectroscopy with Electrons, Forschungszentrum Jülich GmbH, 52425 Jülich, Germany

[3]The School of Electronic and Information Engineering, State Key Laboratory for Mechanical Behavior of Materials, Xi'an Jiaotong University, Xi'an 710049, China

[4] Institute for Theoretical Solid-State Physics, JARA-FIT and JARA-HPC, RWTH Aachen University, 52074 Aachen, Germany

[5] Institute of Physics IA, JARA-FIT and JARA-HPC, RWTH Aachen University, 52074 Aachen, Germany

[6] Department of Materials Science and Engineering, Johns Hopkins University, Baltimore, MD 21218, USA

[7] Peter Grünberg Institute (PGI 10), Forschungszentrum Jülich GmbH, 52425 Jülich, Germany

Corresponding Authors:

* (W.Z.) Email: wzhango@mail.xjtu.edu.cn

‡ These authors contributed equally.

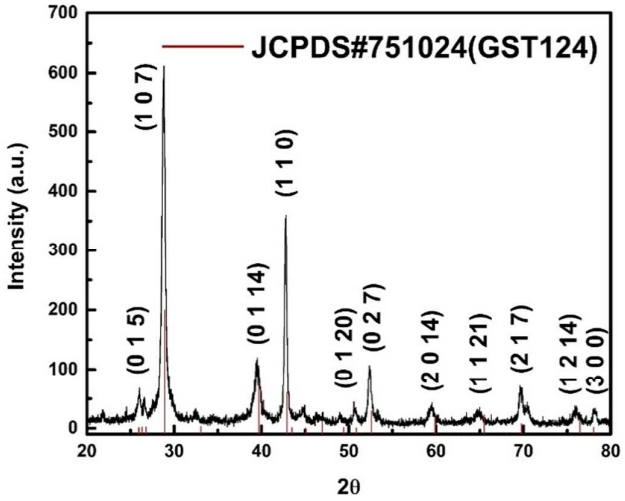

Figure S1. XRD analysis of hexagonal $GeSb_2Te_4$ thin films. All of the detected peaks match well with the JCPDS card of hexagonal $GeSb_2Te_4$ (red lines).

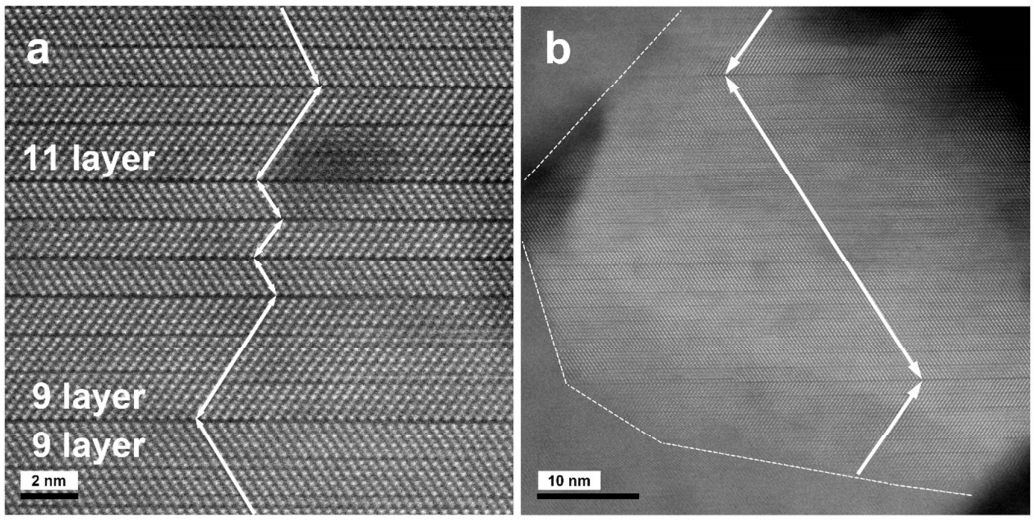

Figure S2. HAADF-STEM images of inverted blocks. White arrows indicate the directions of atomic blocks. The length of the inverted slabs can vary from one (see **a**) to several tens of atomic blocks (see **b**), and the size of atomic blocks can also vary from quintuple to hendecuple. These inverted blocks and slabs can appear anywhere in the samples, both at the center of each grain (see **a**) and near the grain boundary (see **b**, the boundary is marked with dash lines). In short, no clear pattern can be found, owing to the very small energy costs of the different stacking sequence "abc" versus "acb" inside the atomic blocks.

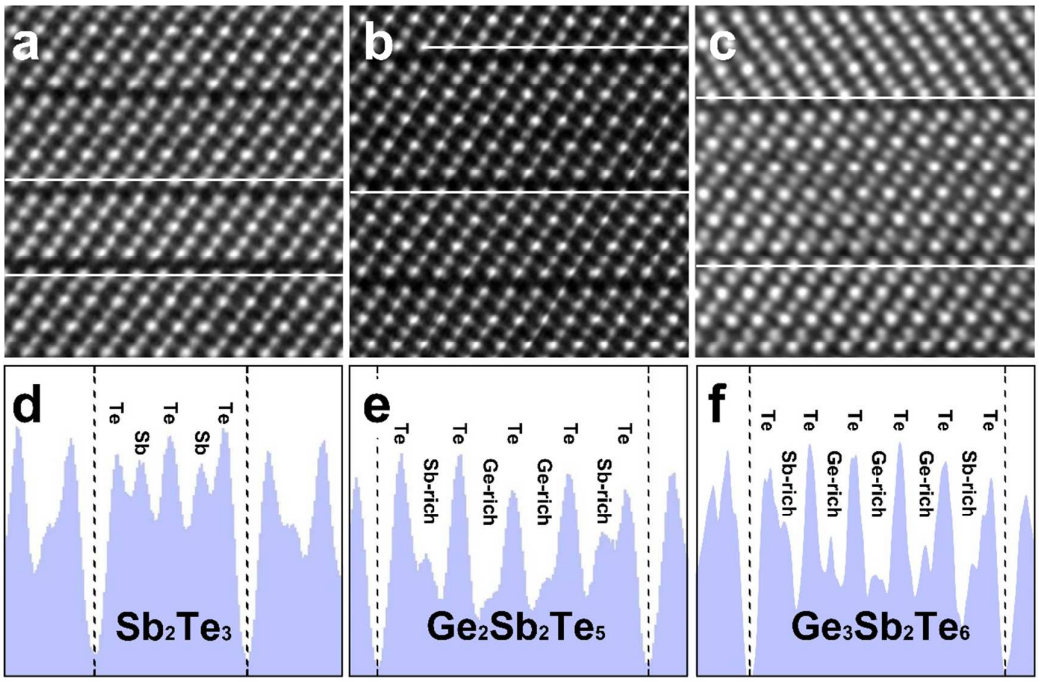

Figure S3. HAADF-STEM images and intensity profiles of various atomic blocks. a-c The HAADF images and d-f the corresponding intensity profiles of atomic blocks of different size, i.e. quintuple-layer, nonuple-layer and hendecuple-layer blocks, which are identified as Sb_2Te_3, $Ge_2Sb_2Te_5$ and $Ge_3Sb_2Te_6$ blocks, respectively.

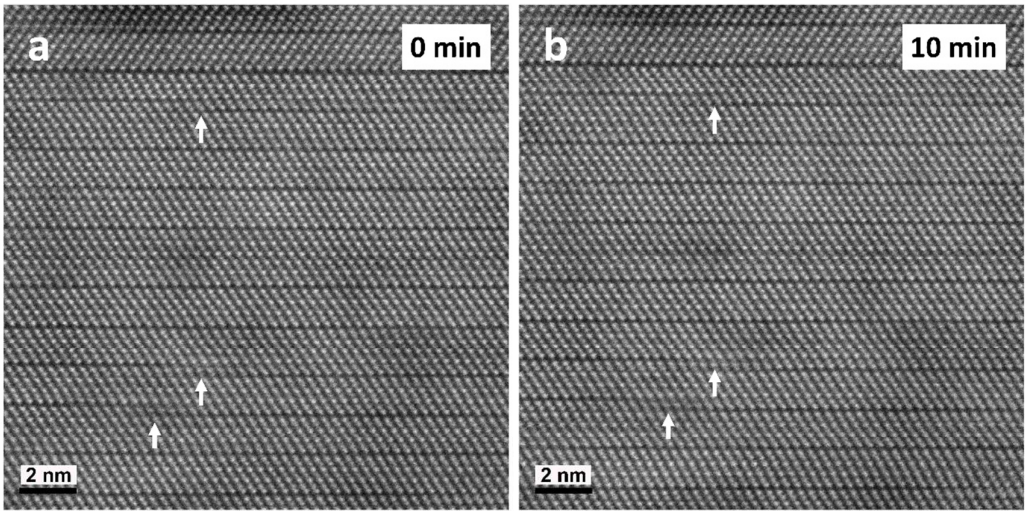

Figure S4. Bi-layer defects under electron beam exposure. The typical data recording time is 1-2 minutes or less. To verify that there is nothing changed under unfocused electron beams, we exposed the bi-layer region under STEM preview model up to 10 minutes, and no obvious structural changes were observed. The diameter of focused electron beams done by A. Lotnyk et al. in Ref. [23] in main text is of the order of approximately 70 pm, which is not used in standard STEM experiments.

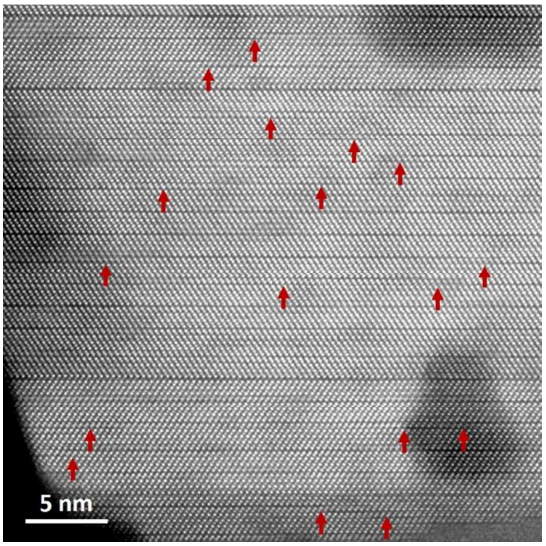

Figure S5. A typical large-scale HAADF scan of bi-layer defects. The red arrows indicate the bi-layer defects. The planar density is determined to be one bi-layer per ~75 nm² through a few hundreds of such HAADF scans.

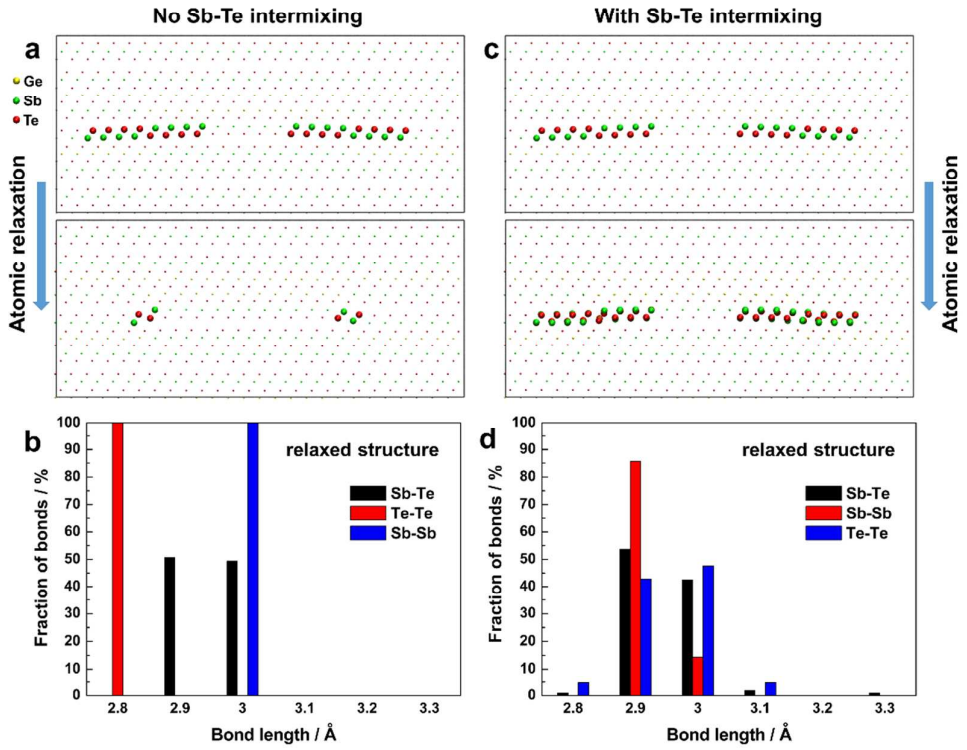

Figure S6. Modelling and intermixing disorder analysis of bi-layer defects. a-b Before and after relaxation, the atomic models with non-mixed and Sb-Te intermixed bi-layer defects, respectively. Atoms in the crossing regions are enlarged. c-d The corresponding fractions of Sb-Te, Sb-Sb and Te-Te bonds in the

bi-layer regions in both relaxed models are counted.

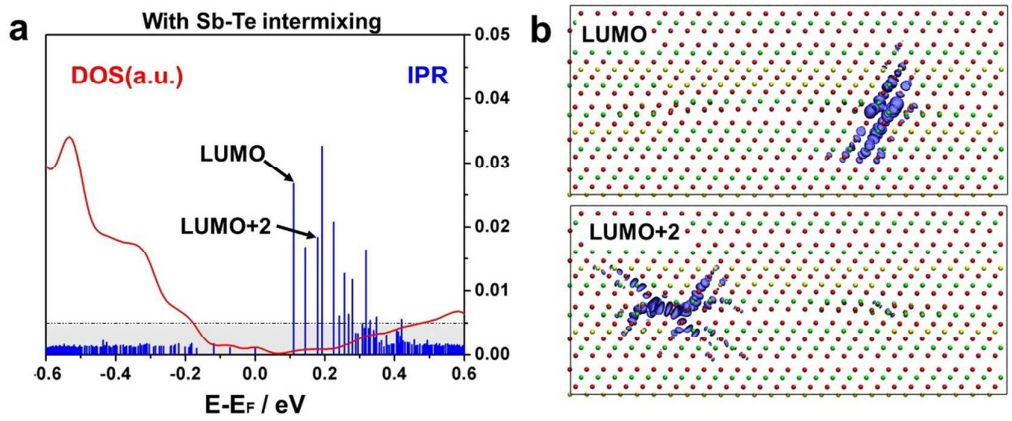

Figure S7. Localization properties of the Sb-Te intermixed bi-layer model. a The DOS and IPR, and b the corresponding lowest unoccupied molecular orbital (LUMO) and LUMO+2 states rendered with the isovalue of 0.01 a.u. The localization is mainly found around the bi-layer defects.